Available online at www.sciencedirect.com
SCIENCE DIRECT
Catalysis Today 105 (2005) 448–454
CATALYSIS TODAY
www.elsevier.com/locate/cattod

Biofilm growth pattern in honeycomb monolith packings: Effect of shear rate and substrate transport limitations

S. Ebrahimi [a,b,*], C. Picioreanu [a], J.B. Xavier [a], R. Kleerebezem [a], M. Kreutzer [c], F. Kapteijn [c], J.A. Moulijn [c], M.C.M. van Loosdrecht [a]

[a] Department of Biotechnology, Delft University of Technology, Julianalaan 67, 2628 BC Delft, The Netherlands
[b] Chemical Engineering Department, Sahand University of Technology, Tabriz, Iran
[c] Reactor and Catalysis Engineering Group, Department of Chemical Engineering, Delft University of Technology, Julianalaan 136, 2628 BL Delft, The Netherlands

Abstract

Potential application of monolith reactors in a biological process was investigated experimentally. A possible problem when using monolith reactors in biological applications is clogging due to biofilm formation. An interesting phenomenon is the pattern in which biofilms develop inside the monolith channels. Rather unexpectedly at a first glance, it was repeatedly observed that biofilm formation started in the middle of a side of the square-section monolith channels, instead of colonizing first the low-shear areas in the corners. To explain this biofilm formation pattern, a two-dimensional mechanistic model based on substrate diffusion and consumption accompanied by microbial growth and detachment was developed in this study. Simulation results suggest that the unexpected biofilm patterns are generated by the balance between biofilm growth and biofilm detachment due to shear stress induced erosion. In the early stages, the biofilm growth in the corners is strongly limited by the external resistance to substrate transfer. As time passes and the biofilm grows in thickness, mechanical forces due to passing gas bubbles will lead to a more regular biofilm shape, including the channel corners.

Keywords: Biofilm; Hydrodynamics; Mathematical modelling; Microorganism; Monolith

1. Introduction

The structure of a monolith reactor consists of a large number of narrow, straight and parallel flow channels. The most important advantages of the monolith reactors are the large open frontal area, resulting in very little resistance to flow and hence low pressure drop and energy loss. The pressure drop in monolith is an order of magnitude lower than in random packed beds [1]

The hydrodynamic behavior of gas–liquid flow in the monolith reactor and the basic mass transfer characteristics for monolith systems have been studied within the context of chemical reaction engineering [2–4]. Monolith columns can be operated in co- or countercurrent with regard to the gas and liquid stream. Countercurrent operation is characterized by a low-pressure drop, but relatively low k_La values as well. In co-currently operated monolith columns very high gas–liquid (G/L) mass transfer rates can be achieved ($k_La \sim 1\ s^{-1}$) at a minimized amount of power consumed (50–80% of conventional bioreactors). These specific features of the monolith reactors – combined low pressure and high mass transfer characteristics – have drawn the attention toward the application of the monolith reactor in multiphase reaction systems. However, the potential application in biofilm systems has not been explored yet. Herewith, monolith columns have a wide application potential within the field of biological processes. The monolith reactor could be considered to become a competitive alternative to conventional gas–liquid bioreactors such as stirred tanks, packed beds and airlift bioreactors.

The main potential problem of monolith reactors in biological applications is clogging due to biofilm formation.

* Corresponding author at: Swiss Federal Institute of Technology Lausanne (EPFL), Switzerland. Tel.: +41 6935728; fax: +41 6934722.
E-mail address: sirous.ebrahimi@epfl.ch (S. Ebrahimi).

0920-5861/$ – see front matter © 2005 Elsevier B.V. All rights reserved.
doi:10.1016/j.cattod.2005.06.051

Nomenclature

List of symbols

C_S	substrate concentration (g m^{-3})
C_{Sb}	substrate concentration in the bulk liquid (g m^{-3})
C_x	biomass concentration in the biofilm (g m^{-3})
D	diffusion coefficient of substrate (m^2/day)
h	grid element size (m)
HRT	hydraulic residence time (h)
K_s	Monod saturation constant for substrate (g m^{-3})
L	monolith channels size (m)
L_F	maximum biofilm thickness (m)
$m_X^{(p)}$	total mass of biofilm particles (g_{COD} m^{-3} particle)
M_X	maximum total mass of biofilm particles (g_{COD} m^{-3} particle)
n	direction normal to the wall
N	grid element numbers
N_P	number of non-overlapping hard spheres of biomass
$N_{P,0}$	initial biomass particles with mass m_0
q_s^{max}	maximum specific substrate conversion rate (g_S/g_{CODX} day)
r_X	biomass growth rate (g_{COD} m^{-3} s^{-1})
R	biomass particle radius (m)
Y_{sx}	growth yield of biomass on substrate (g_{CODX}/g_S)

Greek letters

Ω	computational domain
Ω_1	bulk liquid sub-domain
Ω_2	diffusional sub-domain
δ_{BL}	distance between the diffusional sub-domain and the biofilm maximum thickness (m)
ρ_X	density of biofilm particles (g_{CODX}/g_S)
Δt	time step

Recently, clogging of monolith bioreactors was experimentally investigated in a pilot-scale monolith reactor [5]. The main objective of this experimental work was to determine if presence and absence of the biofilm formation could be controlled in monolith type reactors. The results indicated that at sufficiently longer liquid residence times, the clogging can effectively be delayed and a stable operation could be obtained. It should be noted that the biofilm formation in the monolith channels is not by definition unwanted. This may enable the operation of the monolith packing as biofilm reactor in specific cases. However, in this particular study, biofilm formation was an unwanted side aspect of cultivation at high concentrations of suspended biomass.

Unexpectedly, the biofilm formation patterns in the monolith channels were rather interesting. The biofilm formation would expect to start from the corners of the square monolith channels if the shear had been the prevailing factor counteracting initial biofilm formation. This behavior would be intuitively expected because shear forces generated by liquid or by passing air bubbles are lower in the corners of the channels, leading to less biofilm erosion (detachment). However, in all the experiments it was observed that biofilm formation started from the middle of all faces of the monolith channels. It is known that biofilm formation is the result of a balance between microbial growth supported by substrate transport, and biofilm detachment due to, for example, mechanical forces [6,7]. Therefore, it was hypothesized that the substrate limitation in the corner of monolith channels would be the main reason of this initial biofilm formation pattern, and not the shear forces. To evaluate this hypothesis, the biofilm formation pattern in the monolith channels was simulated by using an individual-based biofilm model. The model including substrate diffusion, reaction and microbial growth [8], supplemented with a detachment mechanism [9], was originally developed for biofilm development on planar solid surfaces. In this study, the two-dimensional biofilm model was adapted to represent a cross section of the square channel.

In this contribution, an overview of the experimental results of the effect of biomass in monolith reactors with respect to biofilm formation and clogging is given. Following, the basis and the results of mathematical modeling on biofilm formation patterns in monolith channels is presented.

2. Experimental investigation

2.1. Objectives

The formation of biofilms in monolith reactors can either be regarded as an unwanted side effect or an operational requirement, depending on the treatment objectives to be met. Operation as biofilm reactor is desired if uncoupling of the solid and liquid retention time is required. In case of sufficiently long liquid retention times the formation of biofilms can be regarded as an unwanted side effect that may increase the pressure drop and decrease the mass transfer rates. Competition between biomass that preferentially resides in a biofilm and biomass that prefers to grow in suspension can be influenced by the hydraulic retention time (HRT). At low HRT-values (HRT $< 1/\mu^{max}$, where μ^{max} is the maximum specific growth rate, h^{-1}) suspended growth cells are washed-out from the system and growth is favored of biomass that is capable of biofilm formation, whereas at long HRT-values (HRT $> 1/\mu^{max}$) growth of suspended bacteria is favored.

The principal objective of the experimental work was to determine if biofilm formation and maintenance could be

controlled in monolith type reactors. The operational variables, which were investigated were the hydraulic residence time (calculated based on total liquid volume in the system), substrate loading rate and the biomass concentration in the system.

2.2. Materials and methods

Experiments were conducted in short monolith packings, length 35 cm and diameter 10 cm obtained from Corning Inc., New York. The monoliths were made by extrusion of cordierite, a ceramic material specially tailored for the application in exhaust cleaning. The porous cordierite has pores or pockets of several microns, which form excellent anchoring places for the attachment of biofilm. The monolith channels was square with a diameter of about 2.98 mm, are termed as 50 cells per square inch (cpsi). The monolith column was placed in a Plexiglas column and silicone kit glue was used to fit the monolith inside the Plexiglas column to prevent a by-pass of gas or liquid. A schematic representation of the reactor-separator system is given in Fig. 1. The reactor was operated continuously for gas and liquid in a cocurrent operation. Influent liquid was distributed at the top of the monolith by means of a spray nozzle. A vessel with a liquid volume of 7 L was used to separate gas–liquid at the bottom of the reactor. Liquid was circulated with a centrifugal pump from gas–liquid separator to the top of the reactor. The temperature was maintained at 30 °C by means of a thermostated water coil placed inside the gas–liquid separator vessel. The pH was controlled at 7 using 4 M NaOH and 4 M H_2SO_4 solutions with an automated pH control system (Applikon, Schiedam, The Netherlands). Mass flow controllers set the flow rate of air and the liquid flow rate was measured by a flow meter. Gas flow rate was 4.2 m^3/h, corresponding to a superficial gas velocity of 0.15 m/s and liquid recirculation rate was 3.6 m^3/h. The pressure drop over the monolith was measured using a differential pressure transmitter connected to the top and bottom of the monolith bed. Then the signal was recorded by a data acquisition system. Glucose was used as a substrate and aerobic heterotrophic biomass from a sequencing batch airlift reactor was used as inoculums [10].

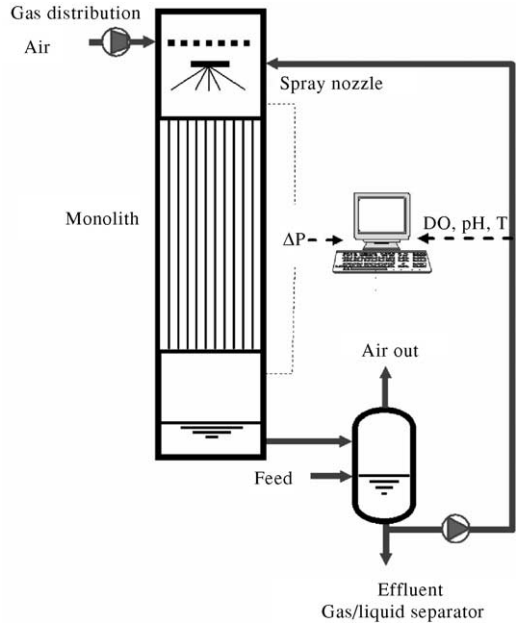

Fig. 1. Experimental setup used for investigation of the biofilm formation in the monolith reactor.

The nutrient feed solution feed was set corresponding to the intended hydraulic residence times. The reactor was operated in non-sterile conditions and a natural mixed culture developed.

3. Experimental results

Results of experimental work have already reported by Ebrahimi [5] and they can be summarized as follows.

3.1. Long liquid residence time

The hydraulic residence time of 30 h is long enough to keep heterotrophic growing microorganisms in the system in a suspended form. Therefore, biofilm growth is expected to be prevented or delayed. Experimental results indicate that, after several weeks, the pressure drop started to rise due to biofilm formation in the monolith channels and then finally a sharp increase in pressure drop was observed. With a glucose feed of 10 and 20 g/L, after 26 and 17 days, respectively, the pressure drop increased very fast, indicating clogging. The resultant biomass concentration in the reactor amounted approximately 5 and 10 g/L when concentration of glucose in the influent was 10 and 20 g/L, respectively. The glucose-grown biofilm in the monolith channels could readily be removed by rinsing with tap water at normal pressure. After cleaning the monolith, the experiment was continued, and essentially the same operating time was obtained. Therefore, it can be concluded that by regular washing of the monolith a long stable operation is possible. It should be noted that in this work, the worse conditions were used with respect to clogging. That is, fast growing heterotrophic bacteria were cultivated on glucose, which is an easily degradable substrate leading to large biomass amounts in a relatively short time.

3.2. Short liquid residence time

By applying a shorter hydraulic residence time (HRT = 0.5 h), the conditions were favorable for biomass to grow in a biofilm rather than in suspension. In these conditions, at the same loading rate as in the long residence time experiments (glucose feed concentration of 0.32 and 0.64 g/L), within a few hours (typically between 5 and 10 h), a sharp increase in pressure drop indicated extensive biofilm growth and eventually channel clogging.

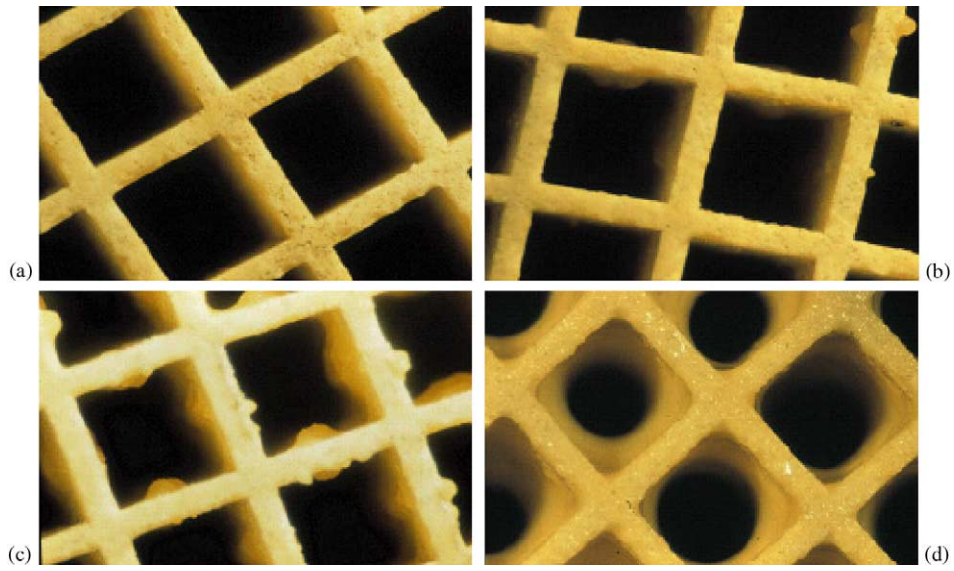

Fig. 2. Photographs of the biofilm developed in the square monolith channels at HRT = 30 h at four moments in time: (a) initial; (b) 7 days; (c) 14 days; and (d) 23 days. The size of the square channel wall is 2.98.

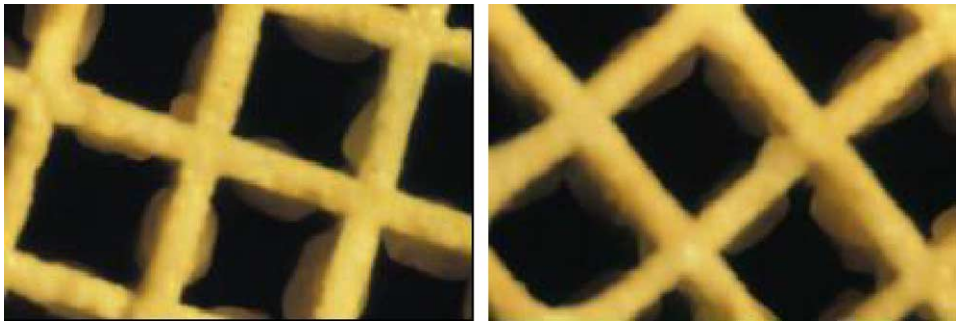

Fig. 3. Photographs of the biofilm developed in the square monolith channels at HRT = 0.5 h, One channel has a diameter of 2.98 mm.

3.3. Biofilm growth pattern in the monolith channels

In the long-term experiments, the monolith was removed every week from the reactor for about 2 h and the shape of the biofilm was photographed under a low magnification microscope. Some of the pictures taken during the experiments at the feed substrate concentration of 20 g/L are shown in Fig. 2. In Fig. 3 a picture taken at the short-term experiments in the end of experiments is shown.

Because shear forces are lower in the corner, the biofilm formation would expect to start from the corner of the monolith channels if the shear had been the prevailing factor inhibiting biofilm formation. However, in all the experiments it was observed that biofilm formation started from the middle of monolith channels. Therefore, it was hypothesized that the substrate limitation in the corner of monolith channels would be the main reason of this biofilm formation pattern, not the shear forces. This explanation is schematically presented in Fig. 4. A thick meniscus forms in the corners as the bubbles pass by: the lubricating film is thick in the corners, and, as a result, the biofilm in the corners is starved from substrate. To evaluate this hypothesis, the biofilm formation pattern in the monolith channels was simulated by using a two-dimensional biofilm model based on diffusion and reaction of substrate accompanied by biomass growth.

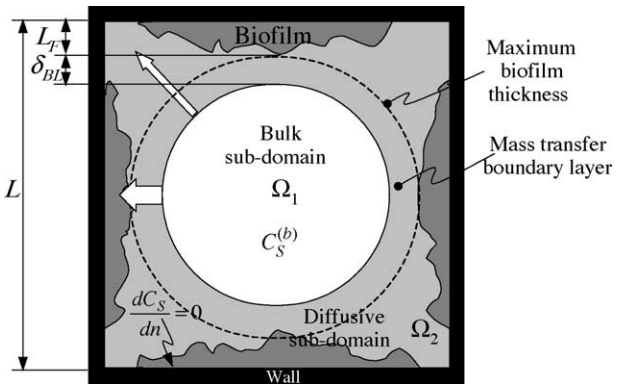

Fig. 4. Schematic representation of the model biofilm system.

4. Mathematical model

4.1. Model description

The model for biofilm formation in square monolith channels is an adaptation of previously biofilm models developed by our group [8,9,11]. Formation of biofilm is simulated in a two-dimensional space Ω having a square shape with the size L (Fig. 4), representing the cross-section of one of the monolith channels. Biofilm development starts with a few initial cells placed on all four sides of the square domain, the sides being the monolith channel walls. The computational domain Ω consists of two sub-domains, Ω_1 and Ω_2. The *bulk liquid sub-domain* Ω_1 is an area of circular shape, considered completely mixed and therefore of uniform concentration of solutes. The soluble substrate concentration in the bulk liquid Ω_1 is $C_S^{(b)}$ (g m^{-3}). For simplicity, it is here considered only one limiting soluble substrate S and one biomass type denoted X, and that neither biological activity nor other reactions are considered in the bulk liquid. The *diffusional sub-domain* Ω_2 contains the rest of the square channel, that is the biofilm itself and a mass transfer boundary layer. The limit of the diffusive sub-domain Ω_2 is the circular bulk liquid sub-domain situated at a distance δ_{BL} from the biofilm maximum thickness L_F (Fig. 4). Diffusion is the only transport mechanism of solutes within Ω_2.

The two-dimensional biofilm model developed in this study contains the following key processes.

4.1.1. Biomass growth

The 2-D biofilm structure is represented by a collection of N_P non-overlapping hard spheres of biomass, also called biomass particles. Each spherical particle p contains only one type of active biomass. It is assumed that each particle has the total mass $m_X^{(p)}$ (g_{COD}/particle) and a constant density of ρ_X (g_{COD} biomass m^{-3} particle). When the biomass in the particle changes in time, volume and radius $R^{(p)}$ change accordingly. The biomass growth in time is described by an ordinary differential equation $dm_X^{(p)}/dt = r_X$, representing the mass balance for each biomass particle p. The net reaction rates for generation of biomass, r_X, are typically functions of the biomass of the particle, $m_X^{(p)}$, and concentrations $C_S^{(x,y,z)}$ of various substrates present at the center (x, y, z) of the biomass sphere. At time $t = 0$, there are $N_{P,0}$ initial biomass particles with mass m_0 and, correspondingly, radius R_0, distributed on all four channel walls.

4.1.2. Biomass division and propagation rules

Due to substrate consumption, the bacterial mass contained in each particle will grow in time. However, the total biomass in a particle is assumed limited to a maximum value, $m_X < M_X$ (g_{COD} biomass m^{-3} particle). M_X is conveniently chosen to achieve the desired total biomass density in the floc $C_{X,max}$ (g biomass m^{-3} floc). When this maximum biomass M_X in a sphere is reached, a new ''daughter'' sphere is created. Half of the biomass contained in the ''mother'' is redistributed to the ''daughter'' sphere, touching the ''mother'' sphere in a randomly chosen direction. Details about the implementation of this division mechanism can be found in [8,11].

4.1.3. Biomass spreading

The biomass spreading in space occurs by shoving the biomass particles when they get too close to each other. The pressure building up due to biomass growth is relaxed by minimizing the overlap of spheres. The monolith walls bounce back biomass particles, thus keeping the biomass within the square channel. This mechanism is explained in detail in [8,11].

4.1.4. Biomass detachment

Detachment is implemented according to the model described in [9]. The detachment function leading to biofilm erosion decreases with the square root of the distance from the channel middle point. Although still crude, this

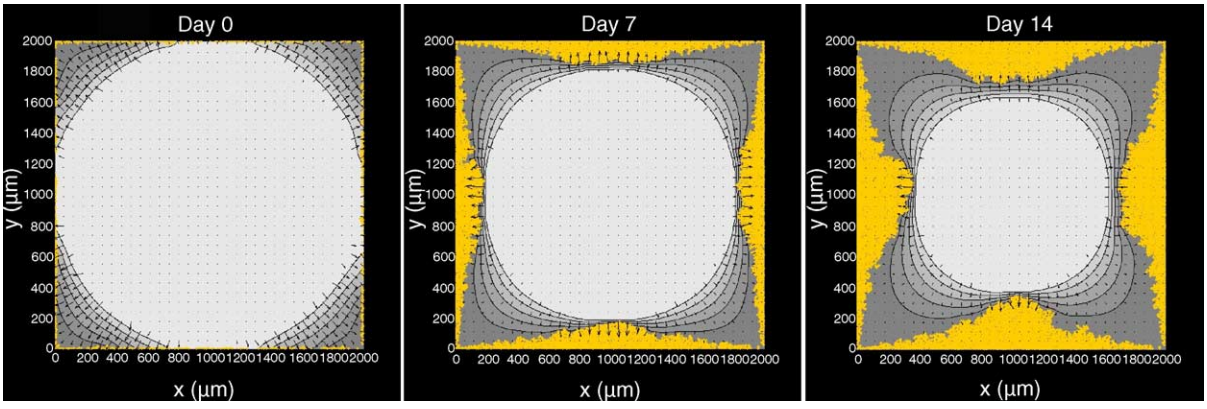

Fig. 5. Simulated development in time of the biofilm in square monolith channels (days 0, 7, and 14, respectively). Substrate concentration field is shown by contour lines and by gray areas with a shade gradually changing from white (maximum concentration) to dark gray (minimum concentration). Arrows represent substrate fluxes and the arrow length is proportional with the flux value. It can be clearly seen that the top of biofilm structure in the middle of the channel wall receives larger substrate fluxes, this leading to larger biomass growth rates than in the corners.

mechanism simulates liquid shearing effects on the biofilm surface. All the removed biomass particles are not relocated but merely considered lost.

4.1.5. Mass balances of soluble substrates

The spatial distribution (''the field'') of concentrations of a given set of substrates influences the growth rate of a particular biomass type. Conversely, the spatial distribution of bacterial activity affects the substrate concentration fields. Due to growth, division, spreading and detachment, the spatial distribution of biomass varies in time. This causes a temporal variation of the substrate fields as well. For this reason, a dynamic diffusion-reaction mass balance must be written for the limiting substrate S substrate in the sub-domain Ω_2:

$$\frac{\partial C_S}{\partial t} = D\left(\frac{\partial^2 C_S}{\partial x^2} + \frac{\partial^2 C_S}{\partial y^2} + \frac{\partial^2 C_S}{\partial z^2}\right) + r_S \tag{1}$$

In Eq. (1) r_S is the net reaction rate and D the diffusivity of substrate. For simplicity, the same diffusion coefficient is considered both in liquid and in biofilm. The net reaction rate of substrate is in this case simply the rate of substrate consumption:

$$r_S = -q_S^{max}\frac{C_S}{K_S + C_S}C_X \tag{2}$$

Accordingly, the rate of biomass production is:

$$r_X = Y_{XS}\, q_S^{max}\frac{C_S}{K_S + C_S}C_X \tag{3}$$

Because concentrations are considered constant in time and uniform in space in the bulk liquid sub-domain Ω_1, the mass balance Eq. (1) does not need to be solved in Ω_1. The boundary conditions for Eq. (1) solved in the diffusional sub-domain Ω_2 consist of: (a) constant substrate concentrations at the interface with the bulk, $C_S = C_S^{(b)}$, and (b) no-flux condition at the impermeable walls, $dC_S/dn = 0$ (where n is the direction normal to the wall). The maximum biofilm thickness $L_F(t)$ increases as the biofilm develops in time and therefore the diffusional domain increases accordingly. For the initial state at $t = 0$, a uniform distribution of concentrations $C_S^{(x,y,z)} = C_S^{(b)}$ throughout the whole domain was assumed.

4.2. Model solution

Solution methods for this type of model equations were described in detail in [8,9]. Only the general succession of steps is presented here. After inoculation with a few biomass particles placed on the monolith walls, the field of substrate concentration at steady state $C_S^{(x,y,z)}(t)$ is computed from Eq. (1) with the appropriate boundary conditions. A uniform space discretization in N^2 square grid elements of size $h = L/(N-1)$ is used. The biomass concentration in each grid element ($C_X^{(x,y,z)}(t)$) is needed to evaluate the reaction term in Eq. (1). This is computed from the sum of all biomass particles having the center situated in the square element, divided by the volume h^3. The concentration fields are used for the solution of biomass balances for each particle, which are integrated directly for one time step Δt to find $m_X^{(p)}(t + \Delta t)$. Division of biomass is executed for those particles which mass exceeds the threshold, i.e., when $m_X^{(p)}(t + \Delta t) > M_X$. Spreading according to the shoving mechanism is then necessary, followed by the detachment of particles. After some of the particles are removed in the detachment step, the biomass dynamics in the time interval Δt has been completed, and a new substrate field needs to be computed.

4.3. Model results

Although a very simplified representation of the reality, the mathematical model still captures the essential features of biofilm formation in square monolith channels. Fig. 5, shows simulation result of the biofilm development in square monolith channels. The parameters used for simulations were as follows:

$$L = 2 \times 10^3\ \mathrm{m}; \quad C_{Sb} = 20\ \mathrm{g/L}; \quad K_s = 1\ \mathrm{g/L};$$
$$q_s^{max} = 2\ \mathrm{g_S/g_{CODX}\ day},\ Y_{sx} = 0.5\ \mathrm{g_{CODX}/g_S}, D = 5 \times 10^5\ \mathrm{m^2/day},$$
$$C_x = 80\ \mathrm{g/L}, \quad \text{and} \quad \delta_{BL} = 40 \times 10^{-6}\ \mathrm{m}$$

Fig. 5 shows that the biomass situated in the middle of the wall (for example at $x = 1000\ \mu m$) will receive larger substrate fluxes. Evidently, these larger fluxes are due to the closer proximity of the biomass in the middle to the bulk zone of maximum concentration than of the biomass situated in the corners, which creates a smaller diffusional path for the substrate molecules. Larger biomass growth rates are then expected in the middle than in the corners, creating biofilm structures qualitatively resembling those experimentally observed in Fig. 5, in the first two weeks of reactor operation. More simulation results and an animation of the biofilm development in time can be found on the web site: http://www.biofilms.bt.tudelft.nl/material.html.

5. Conclusions

Preliminary results indicate that the monolith reactor is a promising concept as a suspended growth bioreactor in biological processes. The experimental results demonstrated that at sufficiently high liquid residence times the clogging can effectively be delayed for several weeks, even at moderately high biomass concentrations as high as 10 gDW/l. Eventually clogging occurs, but biofilms formed can readily be removed by rinsing with tap water. Simulation results of the mathematical model of biofilm development,

based on substrate diffusion-reaction and biomass growth, confirm the substrate limited growth as the main cause of the unexpected biofilm formation pattern.

References

[1] J.J. Heiszwolf, et al. Hydrodynamic aspects of the monolith loop reactor, Chem. Eng. Sci. 56 (3) (2001) 805–812.
[2] J.J. Heiszwolf, et al. Gas–liquid mass transfer of aqueous Taylor flow in monoliths, Catal. Today 69 (1–4) (2001) 51–55.
[3] A.K. Heibel, F. Kapteijn, J.A. Moulijn, Flooding performance of square channel monolith structures, Ind. Eng. Chem. Res. 41 (26) (2002) 6759–6771.
[4] M.T. Kreutzer, et al. Mass transfer characteristics of three-phase monolith reactors, Chem. Eng. Sci. 56 (21–22) (2001) 6015–6023.
[5] S. Ebrahimi, R. Kleerebezem, M.T. Kreutzer, F. Kapteijn, J.A. Moulijn, J.J. Heijnen, M.C.M. van Loosdrecht. Potential application of monolith packed columns as bioreactors, control of biofilm formation, Biotechnol. Bioeng., in press.
[6] M.C.M. Van Loosdrecht, C. Picioreanu, J.J. Heijnen, A more unifying hypothesis for biofilm structures, FEMS Microbiol. Ecol. 24 (2) (1997) 181–183.
[7] M.C.M. van Loosdrecht, et al. Biofilm structures, Water Sci. Technol. 32 (8) (1995) 35–43.
[8] C. Picioreanu, J.U. Kreft, M.C.M. van Loosdrecht, Particle-based multidimensional multispecies biofilm model, Appl. Environ. Microbiol. 70 (5) (2004) 3024–3040.
[9] J.B. Xavier, C. Picioreanu, M.C.M. van Loosdrecht, A general description of detachment for multidimensional modelling of biofilms. Biotechnol. Bioeng., in press.
[10] J.J. Beun, M.C.M. van Loosdrecht, J.J. Heijnen, Aerobic granulation in a sequencing batch airlift reactor, Water Res. 36 (3) (2002) 702–712.
[11] J.U. Kreft, et al. Individual-based modelling of biofilms, Microbiology 147 (2001) 2897–2912.